Study of chirping Toroidicity-induced Alfvén Eigenmodes in the National Spherical Torus Experiment

M. Podestà[1], R. E. Bell[1], A. Bortolon[2], N. A. Crocker[3], D. S. Darrow[1], E. D. Fredrickson[1], G.-Y. Fu[1], N. N. Gorelenkov[1], W. W. Heidbrink[2], G. Kramer[1], S. Kubota[3], B. P. LeBlanc[1], S. S. Medley[1], H. Yuh[4]

[1] Princeton Plasma Physics Laboratory, Princeton NJ 08543 - USA

[3] University of California, Irvine, CA 92697, USA

[2] University of California, Los Angeles, CA 90095, USA

[4] Nova Photonics, Princeton NJ 08543, USA

E-mail: mpodesta@pppl.gov

Abstract.

The National Spherical Torus Experiment (NSTX, [M. Ono *et al.*, Nucl. Fusion **40**, 557 (2000)]) operates with neutral beam (NB) injection as the primary system for heating and current drive. The resulting fast ion population is characterized by velocities up to five times larger than the Alfvén velocity, which provides a strong drive for toroidicity-induced Alfvén eigenmodes (TAEs). TAEs exhibit repeated bursts in amplitude and down-chirps in frequency. Eventually, so-called TAE *avalanches*, which cause large (up to 30%) fast ion losses over $\sim$ 1 ms, are observed. In addition, other modes satisfying the frequency and mode number matching conditions for quadratic coupling among TAEs are detected during avalanches. This indicates that non-linear coupling between modes is at play. The coupling involves other low-frequency MHD modes, such as kink-like modes. The evolution of frequency, amplitude and radial structure of TAEs and low-frequency modes is investigated through a multi-channel reflectometer system. The measured properties are in reasonable agreement with solutions from the ideal MHD code NOVA.

1. Introduction

The enhanced fast ion transport caused by multiple toroidicity-induced Alfvén eigenmodes (TAEs [1]) is believed to be one of the main loss mechanisms for fast ions in ITER [2]. Enhanced losses reduce the fusion efficiency and may cause harm to in-vessel structures. Understanding this phenomenon in present devices in order to limit, or possibly avoid, its deleterious effects in future fusion reactors is therefore paramount for fast ion research [3]. A scenario of concern for ITER is represented by the overlap of multiple TAE resonances in phase space [4]. For sufficiently strong overlap, broad regions of the fast ion distribution function provide free energy to sustain an explosive growth of the instabilities [5]. Modifications of the fast ion phase-space, possibly enhanced by resonance overlap, has been invoked to explain TAE splitting into multiple branches [6], or periodic variations of the frequency (*chirps*) [7][8]. These rapid events are characterized by short time scales, $\lesssim$ 1 ms, for which no possibility of *external*

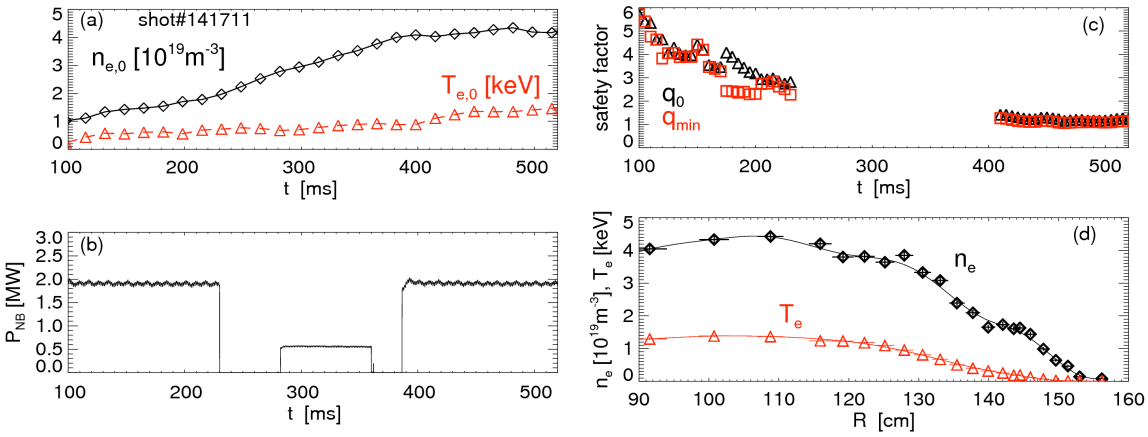

Figure 1. (a) Evolution of density and electron temperature at the magnetic axis for NSTX discharge no. 141711. (b) Waveform of the injected neutral beam power. (c) Evolution of the central and minimum values of the safety factor, q_0 and q_{min}. No data is available for $t = 250 - 410$ ms. (d) Electron density and temperature at $t = 470$ ms. The magnetic axis is at $R \approx 105$ cm.

control (e.g. through tailored injection of neutral beams or rf waves) presently exists. Therefore, they are a particularly challenging issue for future devices.

Typical scenarios on the National Spherical Torus Experiment (NSTX) [9] are considerably different from those predicted for ITER and future fusion devices. Nonetheless, they provide a good test case to improve the present understanding of the basic physics of bursting TAEs. TAE bursts with duration ~ 1 ms are commonly observed in NSTX neutral beam-heated plasmas and can cause up to 30% loss of the confined fast ion population in a single event [10][11]. NSTX plasmas are therefore an excellent test case to challenge present theories and numerical codes, with the overall goal of improving predictive capabilities for applications to future devices. Comparisons between experiments and codes are usually done in terms of the modes' properties (*i.e.* frequency, mode number and radial structure) and of the mode dynamics for varying plasma conditions. A detailed characterization of the radial structure of the TAE and of its eventual modifications during the bursting/chirping phase, is the main goal of this paper. Previous results have also shown that mode-mode coupling is at play during large TAE bursts [12]. As a result of three-wave interactions, low-frequency ($\lesssim 30$ kHz) modes with toroidal mode number $n = 1$ are observed, which are responsible for further enhancement of the fast ion and thermal plasma transport. The nature of this low-frequency fluctuation is also discussed in this paper. The paper is organized as follows. The experimental scenario used for TAE studies on NSTX is summarized in Sec. 2. General observations on TAE dynamics are presented in Sec. 3. The evidence of coupling between TAEs and low-frequency MHD modes is discussed in Sec. 4. Section 5 summarizes the main finding of this work.

2. Experimental scenario

NSTX operates with a toroidal field ~ 0.5 T, with typical density $3 - 10 \times 10^{19}$ m^{-3}, temperature $T_e \approx T_i \lesssim 1.5$ keV and central plasma rotation $f_{rot} \lesssim 40$ kHz. Neutral beam (NB) injection is the main heating system. The maximum total power is $P_{NB} = 7$ MW from three sources with adjustable

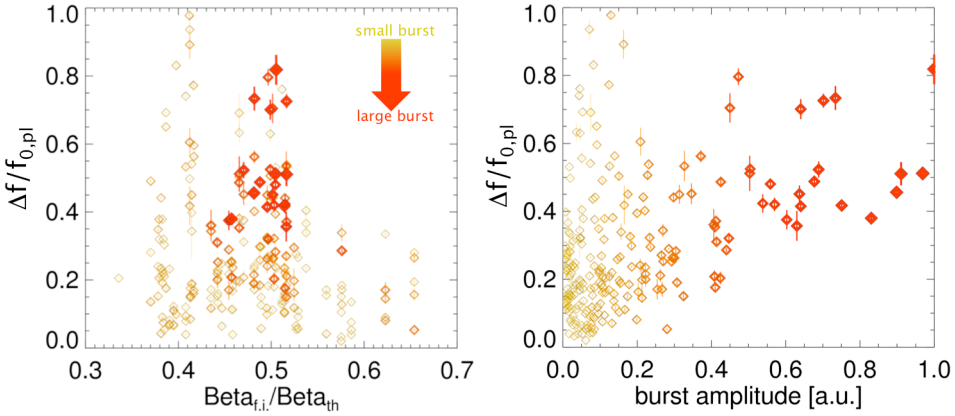

Figure 2. Parameter space for bursting/chirping TAEs in L-mode. Shown is the relative frequency variation, normalized to the mode frequency in the plasma frame, with respect to the ratio of central fast ion to plasma β (left) and amplitude increase during the frequency chirp (right). Mode amplitudes typically measured by Mirnov coils at the plasma edge are $\delta B/B \sim 10^{-4}$ (corresponding to ~ 0.1 in the normalized units of burst amplitude in the left figure), which can increase by for the larger bursts.

injection energy $E_{inj} = 60 - 90$ keV. The resulting fast ion population is super-Alfvénic with velocities $1 < v_{fast}/v_{Alfven} < 5$. Fast ions provide the drive for a variety of Alfvénic instabilities, including TAEs [13]. The latter have toroidal mode number up to $n = 8$ and frequency $60 < f < 250$ kHz in the laboratory frame. An example of the L-mode plasma scenario used for TAE studies is shown in Fig. 1. Deuterium plasmas with $1 - 2.5$ MW of injected NB power are mainly used. The reversed-shear safety factor profile, $q(R)$, evolves in time. Its minimum, q_{min}, decreases from 4 to ≈ 1 during the discharge (Fig. 1c). The safety factor is reconstructed through the Grad-Shafranov equilibrium code LRDFIT [14], constrained by Motional Stark Effect (MSE) measurements of the magnetic pitch.

3. General characteristics of TAE dynamics

3.1. Frequency and amplitude evolution

Most of the TAE studies on NSTX have been conducted, so far, in NB-heated L-mode plasmas. Because of the relatively low density ($n_e \sim 3 - 4 \times 10^{-19}$ m^{-3}) and magnetic configuration of a spherical tokamak with low toroidal field, $B_t \sim 0.5$ T, these discharges are characterized by a high ratio of fast ion to thermal *beta*'s, $\beta_{f.i.}/\beta_{th}$. Taking the frequency variation as indicative of the severity of a burst, the relationship between measured frequency chirp and $\beta_{f.i.}/\beta_{th}$ is shown in Fig. 2 for a set of discharges with different electron densities and injected NB power. The fractional frequency chirp is calculated with respect to the mode's frequency in the plasma frame. As expected, larger values of $\beta_{f.i.}/\beta_{th}$ correspond, *on average*, to larger frequency chirps and amplitude excursions. However, there is still a considerable fraction of bursts with relatively mild amplitude and frequency excursions. This suggests that the available fast ion drive, which is roughly proportional to $\beta_{f.i.}$, is only one of the parameters regulating the TAE dynamics, as expected for a semi-chaotic regime in which multiple drive and damping terms compete [5][15].

A spectrum of magnetic fluctuations, measured at the low-field side of the vacuum vessel by Mirnov

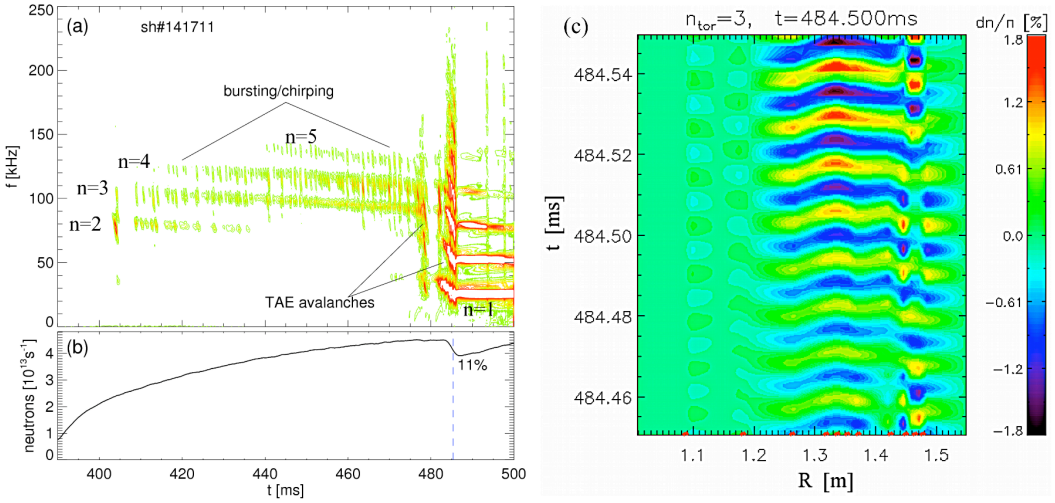

Figure 3. (a) Spectrogram of magnetic field fluctuations from Mirnov coils showing TAEs with different behavior: quasi-stationary modes, bursting/chirping modes and large *avalanches* (some of which are indicated in the figure). (b) Neutron drops associated with TAE avalanches. (c) Example of density fluctuation evolution as reconstructed from a multi-channel reflectometer system for a $n = 3$ mode.

coils for the discharge in Fig. 1, is shown in Fig. 3a. Bursts of TAEs correlate with frequency variations < 10 kHz for $t < 480$ ms. Bursts repeat with a period of $0.5-2$ ms, whose duration is rather independent of thermal plasma parameters or injected NB power. Eventually, larger bursts with frequency down-chirp > 10 kHz lead to a so-called TAE *avalanche* [11]. Avalanches cause significant fast ion losses [10], as inferred from the neutron rate, *cf.* Fig. 3b. (Because the neutron rate is mostly determined by beam-plasma reactions, the relative drop in neutron rate is approximately equal to the fractional depletion in the fast ion population). In addition to TAEs, activity with $n = 1$ and $f \sim 25$ kHz (i.e. well below the TAE gap), along with a weaker $n = 2$ harmonic at twice that frequency, is detected during strong TAE bursts. This fluctuation has a duration comparable with, or larger than, that of the avalanches, indicating that the $n = 1$ fluctuation may also have a role in the fast ion loss process [12].

Another general feature of TAEs in NSTX L-mode plasmas is the roughly constant frequency separation between peaks with consecutive n's [16]. This suggests that the modes share a common frequency in the plasma frame, f_0^{TAE}, such that $f_{lab,n}^{TAE} = f_0^{TAE} + n\, f_{Doppler}^{TAE}$ [17]. Here $f_{lab,n}^{TAE}$ is the frequency for the toroidal mode number n in the laboratory frame and $f_{Doppler}^{TAE}$ the Doppler shift caused by plasma rotation. Knowing $f_{Doppler}^{TAE}$ and the plasma rotation profile $f_{rot}(R,t)$, measured through charge-exchange recombination spectroscopy of carbon rotation [18], the radius R^{TAE} such that $f_{Doppler}^{TAE} = n\, f_{rot}(R^{TAE})$ can be calculated. In the following, R^{TAE} is referred to as the *mode location*. Its importance to understand the mode dynamics is further discussed in Sec. 3.3.

3.2. Mode structure measurements

The TAE dynamics can be explored through the NSTX multi-channel reflectometer system [19], which measures the phase variations of an injected microwave signal resulting from plasma density fluctuations. The system has 16 channels tuned at different frequencies. Depending on the density profile, hence on

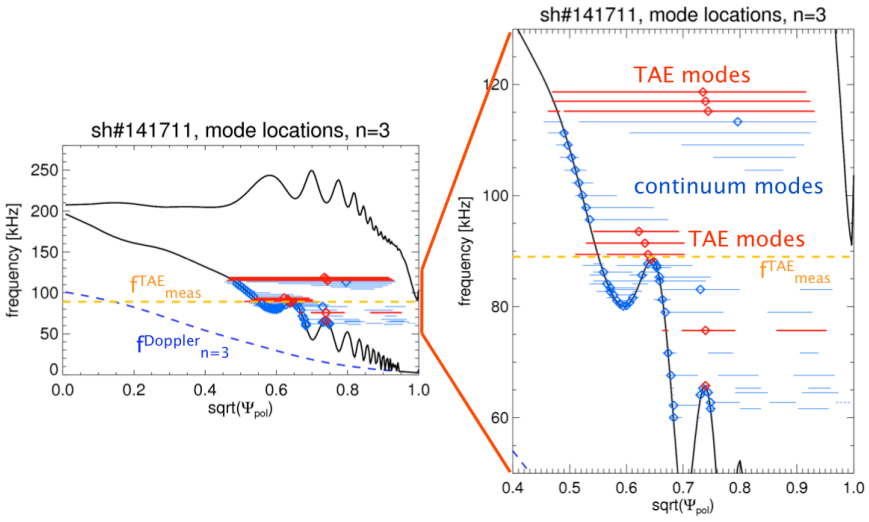

Figure 4. NOVA calculation of the TAE continuum and location of the TAE/RSAE and continuum eigenmodes for $n = 3$. The measured frequency is shown as a dashed line at $f = 89$ kHz.

the location of the cut-off radius for each specific frequency (channel), density fluctuations at up to 16 radial points can be measured. For the L-mode scenario investigated here there are typically $9-11$ radial points available. An example of reconstructed density fluctuations, $\delta n/n$, associated with a $n = 3$ mode at $f \approx 89$ kHz (*cf.* Fig. 3a) is shown in Fig. 3c, showing the potential for $\delta n/n$ measurements at high temporal resolution, as required for transient events such as TAE bursts and avalanches.

The agreement between the measured mode structure and linear MHD models is explored via the NOVA code ([20] and references therein). NOVA calculations of the $n = 3$ TAE continuum at $t = 470$ ms, i.e. just before the TAE avalanche, are shown in Fig. 4. Toroidal rotation is included as a Doppler shift contribution. From the many (ideal) eigenmodes found by NOVA, the best fit to the experimental mode is selected based on the agreement with the measured mode number, frequency and $\delta n/n$ profile, as detailed in Ref. [11]. The result of such procedure is reported in Fig. 5. Apart from a radial shift of $2-5$ cm, the modeled $\delta n/n$ is in fair agreement with the measurements for modes with $n = 2\ldots5$. In turn, poor agreement is found for the low-frequency $n = 1$ mode. The radial shift is likely due to the procedure used to prepare the experimental profiles, processed by the transport code TRANSP [21], for the NOVA input. As a further step, the possible distortion of the mode structure during large bursts is investigated. The mode structure evolution during an avalanche is illustrated in Fig. 6b-e for modes with $n = 2\ldots5$. Data refer to three different times, corresponding to the maximum mode activity of the three consecutive bursts that actually form the avalanche, as seen from the high time resolution spectrogram in Fig. 6a. The reflectometer data show that, in spite of the large amplitude and frequency variations occurring during the avalanche, the mode structure does not vary significantly. Consistently with the model discussed in Ref. [22], the broad radial structure of the modes relative to the scale-lengths of the fast ion density profile is believed to inhibit here a macroscopic radial propagation of the mode.

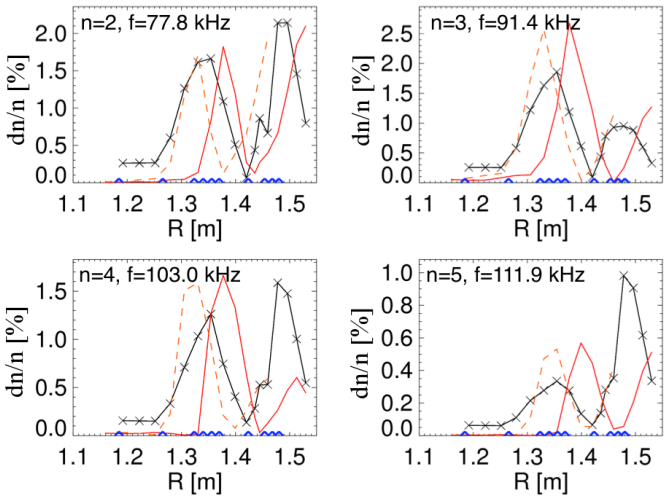

Figure 5. Comparison between $\delta n/n$ measured (solid, cross) and calculated by NOVA (solid,red) for $n = 2 \cdots 5$. Dashed lines are the radially-shifted NOVA solutions that provide the best match with the experiment.

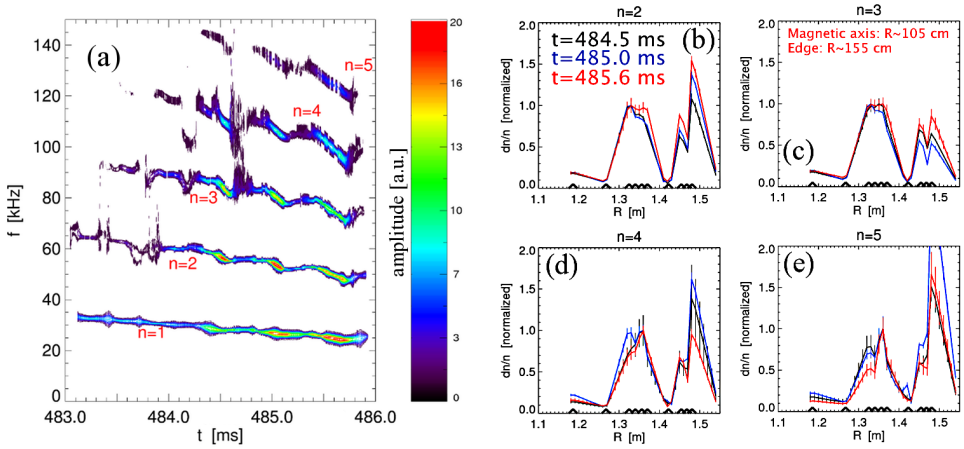

Figure 6. (a) Detail of the frequency and amplitude evolution during a TAE avalanche for discharge no. 141711. (b) Measured $\delta n/n$ at three stages of the burst (right) for $n = 2 \ldots 5$. Amplitudes are rescaled to provide a better comparison for the radial structure.

3.3. Role of fast ion drive

A first example of dependence of mode dynamics on fast ion population is given in Fig. 7, where the fast ion profile is measured under different heating schemes, including NB-only and NB+rf injection. The reference discharge has NB injection only (Fig. 7a). The companion discharges have both NB+rf injection, with a notch of 20 ms in the NB power (Fig. 7b) and in the rf power (Fig. 7c). As the figures show, NB injection alone is insufficient to drive TAEs unstable. When rf is added, the fast ion population slightly increases, as observed from the raise in neutron rate (Fig. 7d), and the modes are destabilized. It is plausible to assume that TAEs remain close to marginal stability, as suggested by the fact that their amplitude drops to noise level as soon as either NB or rf injection is interrupted. A noticeable result is the prompt onset of the bursting/chirping regime, indicating how easily the modes enter in this phase, at least for NSTX plasmas, once they are driven unstable.

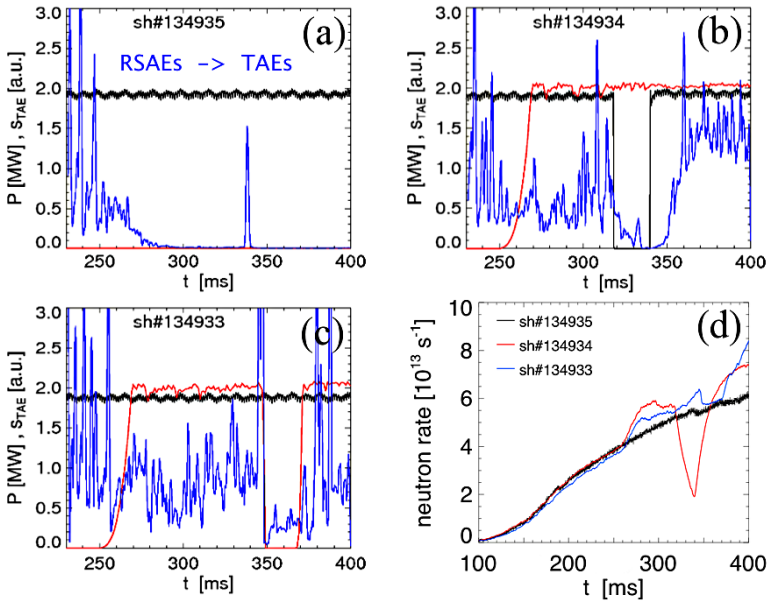

Figure 7. Effect of different heating schemes on TAE dynamics, with (a) NB only, (b-c) NB+rf with a notch in NB and rf power, respectively. Modes before $t \approx 250$ ms are classified as Reverse-shear Alfvén eigenmodes, which then transition into TAEs. (d) Measured neutron rate for the three cases, showing a slight increase in reactivity once rf is turned on.

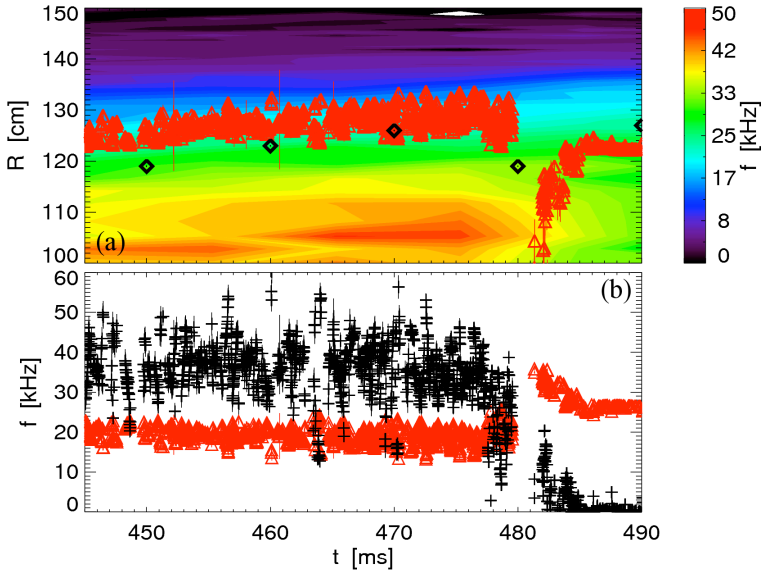

Figure 8. (a) Evolution of toroidal rotation. Black diamonds indicate the position of steepest fast ion gradient. Red triangles show the evolution of R^{TAE}. Note the large shift of R^{TAE} at $t \approx 480$ ms, when a TAE avalanche occurs. (b) Calculated f_0^{TAE} and $f_{Doppler}^{TAE}$ as a function of time. Data from NSTX discharge no. 141711.

A link between mode dynamics and fast ion population can be established experimentally by measuring the fast ion profile and its temporal evolution, *e.g.* through Fast Ion D-Alpha (FIDA) spectroscopy [23][24]. The correlation between TAEs and their drive is discussed in Fig. 8a, where the calculated R^{TAE} (*cf.* Sec. 3.1) is compared with the position of steepest fast ion gradient. The two locations are similar, indicating that the shape of the fast ion profile plays a primary role in determining

the localization (and, possibly, the dynamics) of TAEs. This observations may be used to design tools to affect the fast ion, hence the TAE, dynamics, for instance by varying the NB deposition profile and/or by means of localized rf deposition. (Note that the maximum toroidal rotation shear is also measured at the same radius, although it has been shown that rotation shear does not affect the macroscopic mode dynamics, *cf.* Ref. [16]). The dependence upon the location of steepest fast ion gradient is believed to be responsible for the clustering of multiple modes around the same radius. The strong NB source term can efficiently sustain a steep, localized fast ion gradient, thus paving the way for mutual interactions between strongly unstable modes [12].

A departure of R^{TAE} from the steepest fast ion gradient radius is observed during the avalanche phase around $t = 480$ ms, see Fig. 8a. At this time, the calculated R^{TAE} shifts toward the magnetic axis. Correspondingly, $f_0^{TAE} \rightarrow 0$ and the measured $f_{lab,n}^{TAE} \approx n \times f_{Doppler}^{TAE}$. The proposed interpretation is that the dependence of R^{TAE} on the fast ion profile is partly lost during the avalanche, and the TAEs lock instead on a core-localized mode which starts at the magnetic axis and then move outward in the ~ 10 ms following the TAE burst. This scenario, suggestive of coupling between TAEs and a low-frequency MHD mode, is further investigated in the next Section.

4. Coupling with low-frequency MHD modes

Because of its limitations in temporal resolution and the lack of statistics for events of short duration, Fourier analysis has limited use to study the mode coupling process during single bursts (hundreds of microseconds). Based on the naturally occurring frequency separation between modes, caused by the large Doppler shift $\propto n \times f_{Doppler}^{TAE}$, an analysis based on band-pass filtering of the time series from Mirnov coils is used instead. Signals are band-pass filtered around the frequency of each mode to obtain the corresponding fluctuations, $\dot{s}_n(t)$, and the B-field fluctuation signals, $s_n(t)$ through software integration of $\dot{s}_n(t)$. The evolution of frequency and amplitude, f_n and A_n, are then calculated from the peak-to-peak amplitude and maxima separation of the resulting (sinusoidal) $s_n(t)$.

From a simple model based on bilinear interactions between pairs of modes, the resulting fluctuations can be reconstructed as [12] $\dot{s}_{n_3} =< c_{(n_1,n_2)}\, s_{n_1} s_{n_2} >_{f_{n_3}}$, with the constraints between mode numbers and real frequencies given by $n_3 = n_1 \pm n_2$, $f_{n_3} = f_{n_1} \pm f_{n_2}$. The right-hand side in the equation for $\dot{s}_{n_3}$ is filtered around the frequency f_{n_3} and the dot indicates a time derivative. Note that s_{n_2} is the complex conjugate of the true signal for difference interactions. $c(n_1, n_2)$ represents a coupling coefficient, which is used here as free scaling parameter. For finite damping or growth of the modes, $c(n_1, n_2)$ is a complex quantity [25] whose phase, along with the relative phase between the modes involved in the coupling, determines whether an explosive instability can occur [26]. For the measured signals, $s_n \rightarrow \Re\{s_n\}$ ($\Re\{\ldots\}$ is the real part). In practice, all phase terms, including the relative phase between modes and the phase of the coupling coefficient, will result in a phase, ϕ, between $\dot{s}_{n_3}$ and the reconstructed $< c_{(n_1,n_2)}\, s_{n_1} s_{n_2} >_{f_{n_3}}$. Note that this analysis, performed by using the frequencies measured in the laboratory frame, is valid only if the modes experience the same Doppler shift. If each mode experiences a different Doppler shift, the mode frequencies in the plasma frame, inferred from the actual mode locations and individual Doppler shift frequencies, must be used instead. For this mechanism

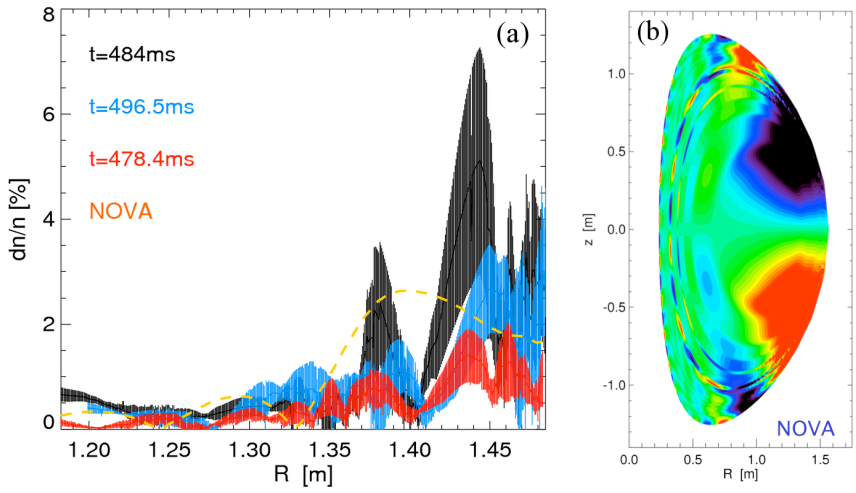

Figure 9. (a) Measured $\delta n/n$ associated with a kink-like mode before ($t = 478.4$ ms), during ($t = 484$ ms) and after ($t = 496.5$ ms) a TAE avalanche. The dashed line is the $\delta n/n$ profile simulated by NOVA, rescaled to match the measured values. (b) Complete two-dimensional profile of density fluctuations as calculated by the linear MHD code NOVA for a $n = 1$ kink-like mode with $f \approx 0$ in the plasma frame.

to be efficient, three-wave matching conditions must be maintained for a sufficiently long time, of the order of tens of wave cycles of the primary (pump) modes, as observed from the experiments .

The validity of this method was demonstrated in Ref. [12], which reports evidence for the coupling between TAE modes and a $n = 1$ fluctuation. The latter was not yet identified in [12]. Based on the upgraded reflectometer system, the density fluctuation resulting from the $n = 1$ mode has been measured (Fig. 9a) and compared with NOVA calculations for ideal kink modes. No solutions are found for the standard, fixed boundary version of the code, which assumes vanishing mode amplitude at the plasma edge (separatrix). When the fixed boundary constraint is removed, a kink mode is found, see Fig. 9b. The mode cause large edge perturbations, which is qualitatively consistent with the experimental observations. This supports the interpretation of the $n = 1$ fluctuation as a kink-like mode. Further studies will include fast ion effects in the simulation to further investigate whether the mode is an ideal kink or a energetic-particle driven fishbone mode.

5. Summary and conclusion

This work has investigated two main aspects of chirping TAE modes on NSTX, namely (i) the mode's properties (e.g. frequency, amplitude, radial structure and some qualitative dependence on the fast ion drive) during the bursting/chirping TAE regime, and (ii) the non-linear coupling between multiple modes leading to the destabilization of low-frequency, kink-like activity.

Chirping parameters are rather constant among different scenarios, characterized by different schemes of additional heating (NB, rf) and confinement mode (L- *vs.* H-mode). Bursting rates are distributed in the range $0.5 - 2$ ms^{-1} with no systematic dependence observed on thermal plasma and fast ion parameters. On average, a tendency of larger bursts/chirps is nevertheless observed for larger fast ion pressures (normalized to the thermal plasma pressure). Through the comparison with the linear

MHD code NOVA, it has been shown that, although even the single-mode dynamics are complex, the mode structure is still reasonably explained in terms of linear eigenmode solutions.

By studying the coupling between pairs of TAEs, we observed that the non-linear, multi-mode TAE dynamic is prone to cause coupling with lower frequency modes, such as $n = 1$ kinks, which mediates the three-wave coupling between primary TAEs [12]. The destabilization of otherwise stable kinks cause fast ion and thermal plasma losses that add to those caused by the TAE modes. The coupling between TAEs is favored by their clustering around a similar radial location. This is plausibly caused by the steep fast ion density gradient sustained at that location by NB injection. Similar conditions could be expected in fusion devices such as ITER. As a result of such non-linear TAE dynamics, an enhancement of fast ion loss or redistribution (in both velocity and real space) is expected. The radial mode extension can be used for a rough guess of whether fast ions are actually expelled or not from the core plasma. Significant losses are likely for global, radially extended TAEs with low n's, whereas more localized TAEs with high n's are more likely to cause redistribution. The latter case is predicted for the high toroidal field, large major radius plasmas of ITER [27]. However, even if no direct loss of fast ions is expected, redistribution itself can be a deleterious process in a reactor. First, modifications of the fast ion distribution may result in unwanted variations of the non-inductive current profile [28]. Second, a relaxed fast ion pressure can impact the stability of other modes (*e.g.* kinks [29], sawteeth [30] and Resistive Wall Modes [31]), thus affecting the overall plasma stability.

Future work will focus on the comparison between the measured mode properties and dynamics and those predicted by both linear (NOVA [20]) and non-linear, self-consistent (M3D-K [32][33]) codes.

Acknowledgments

Work supported by US DOE Contract Number DE-AC02-09CH11466.

[1] CHENG, C. Z., et al., Low-n Alfvén spectra in axisymmetric toroidal plasmas, Phys. Fluids **29** (1986) 3695.

[2] FASOLI, A., et al., Progress in the ITER physics basis: Chapter 5, Physics of energetic ions, Nucl. Fusion **47** (2007) S264.

[3] ZONCA, F., et al., Nonlinear dynamics and complex behaviors in magnetized plasmas of fusion interest, in Frontiers in Modern Plasma Physics, edited by P.K. Shukla, B. Eliasson, and L. Stenflo, volume 34, AIP CP 1061, 2008.

[4] CHIRIKOV, B. V., A universal instability of many-dimensional oscillator systems, Phys. Rep. **52** (1979) 263.

[5] BERK, H. L., et al., Numerical simulation of bump-on-tail instability with source and sink, Phys. Plasmas **2** (1995) 3007.

[6] FASOLI, A., et al., Nonlinear splitting of fast particle driven waves in a plasma: Observation and theory, Phys. Rev. Lett. **81** (1998) 5564.

[7] HEIDBRINK, W. W., Beam-driven chirping instability in DIII-D, Plasma Phys. Control. Fusion **37** (1995) 937.

[8] GRYAZNEVICH, M. P., et al., Beta-dependence of energetic particle-driven instabilities in spherical tokamaks, Plasma Phys. Control. Fusion **46** (2004) S15.

[9] ONO, M., et al., Exploration of spherical torus physics in the NSTX device, Nucl. Fusion **40** (2000) 557.

[10] PODESTÀ, M., et al., Experimental studies on fast-ion transport by Alfvén wave avalanches on the National Spherical Torus Experiment, Phys. Plasmas **16** (2009) 056104.

[11] FREDRICKSON, E. D., et al., Modeling fast-ion transport during toroidal Alfvén eigenmode avalanches in the National Spherical Torus Experiment, Phys. Plasmas **16** (2009) 122505.

[12] PODESTÀ, M. et al., Non-linear dynamics of toroidicity-induced Alfvén eigenmodes on the National Spherical Torus Experiment, Nucl. Fusion **51** (2011) 063035.

[13] MEDLEY, S. S., et al., MHD-induced energetic ion loss during h-mode discharges in the National Spherical Torus Experiment, Nucl. Fusion **44** (2004) 1158.

[14] MENARD, J. E., 2008, private communication.

[15] LILLEY, M. K., et al., Effect of dynamical friction on nonlinear energetic particle modes, Phys. Plasmas **17** (2010) 092305.

[16] PODESTÀ, M., et al., Effects of toroidal rotation shear on toroidicity-induced Alfvén eigenmodes in NSTX, Phys. Plasmas **17** (2010) 122501.

[17] STRAIT, E. J., et al., Doppler shift of the TAE mode frequency in DIII-D, Plasma Phys. Control. Fusion **36** (1994) 1211.

[18] BELL, R. E., et al., Comparison of poloidal velocity measurements to neoclassical theory on NSTX, Phys. Plasmas **17** (2010) 082507.

[19] CROCKER, N. A., et al., High spatial sampling global mode structure measurements via multichannel reflectometry in NSTX, Plasma Phys. Control. Fusion **53** (2011) 105001.

[20] CHENG, C. Z., Kinetic extensions of magnetohydrodynamics for axisymmetric toroidal plasmas, Phys. Rep. 211 **1** (1992).

[21] http://w3.pppl.gov/transp/.

[22] ZONCA, F. E. A., Transition from weak to strong energetic ion transport in burning plasmas, Nucl. Fusion **45** (2005) 477.

[23] PODESTÀ, M., et al., The NSTX fast-ion D-alpha diagnostic, Rev. Sci. Instr. **79** (2008) 10E521.

[24] HEIDBRINK, W. W., Fast-ion D-alpha measurements of the fast-ion distribution, Rev. Sci. Instr. **81** (2010) 10D727.

[25] STENFLO, L., Resonant three-wave interactions in plasmas, Phys. Scr. **T50** (1994) 15.

[26] WILHELMSSON, H., et al., Explosive instabilities in the well-defined phase description, J. Math. Phys. **11** (1970) 1738.

[27] GORELENKOV, N. N., et al., Beam anisotropy effect on Alfvén eigenmode stability in ITER-like plasmas, Nucl. Fusion **45** (2004) 226.

[28] GERHARDT, S. P., et al., Calculation of the non-inductive current profile in high-performance NSTX plasmas, Nucl. Fusion **51** (2011) 033004.

[29] PORCELLI, F., et al., Solution of the drift-kinetic equation for global plasma modes and finite particle orbit widths, Phys. Plasmas **1** (1994) 470.

[30] GRAVES, J. P., et al., Experimental verification of sawtooth control by energetic particles in ion cyclotron resonance heated JET tokamak plasmas, Nucl. Fusion **50** (2010) 052002.

[31] BERKERY, J. W., et al., The role of kinetic effects, including plasma rotation and energetic particles, in Resistive Wall Mode stability, Phys. Plasmas **17** (2010) 082504.

[32] PARK, W., et al., Plasma simulation studies using multilevel physics models, Phys. Plasmas **6** (1999) 1796.

[33] LANG, J., et al., Gyrokinetic ∂f particle simulations of toroidicity-induced Alfvén eigenmode, Phys. Plasmas **16** (2009) 102101.